

# Radiation-Induced Thyroid Stunning: Differential Effects of $^{123}\text{I}$ , $^{131}\text{I}$ , $^{99\text{m}}\text{Tc}$ , and $^{211}\text{At}$ on Iodide Transport and NIS mRNA Expression in Cultured Thyroid Cells

Charlotta Lundh<sup>1</sup>, Ulrika Lindencrona<sup>1</sup>, Per Postgård<sup>1</sup>, Therese Carlsson<sup>2</sup>, Mikael Nilsson<sup>2</sup>, and Eva Forssell-Aronsson<sup>1</sup>

<sup>1</sup>Department of Radiation Physics, Sahlgrenska Academy, Göteborg University, Göteborg, Sweden; and <sup>2</sup>Department of Medical Chemistry and Cell Biology at the Institute of Biomedicine, Sahlgrenska Academy, Göteborg University, Göteborg, Sweden

Recent clinical and experimental data demonstrate that thyroid stunning is caused by previous irradiation and may influence the efficacy of  $^{131}\text{I}$  radiation therapy of thyroid cancer and possibly hyperthyroidism. To avoid stunning, many clinics have exchanged  $^{131}\text{I}$  for  $^{123}\text{I}$  for pretherapeutic diagnostic imaging and dose planning. Furthermore, recent *in vitro* studies indicate that  $^{131}\text{I}$  irradiation reduces iodide uptake by downregulating the expression of the sodium iodide symporter (NIS). The rationale for this study was therefore to study effects on iodide transport and NIS messenger RNA (mRNA) expression in thyrocytes exposed to both  $^{123}\text{I}$  and  $^{131}\text{I}$  in addition to some other potentially interesting radionuclides. **Methods:** Thyrotropin-stimulated thyroid cell monolayers were exposed to 0.5 Gy of  $^{123}\text{I}$ ,  $^{131}\text{I}$ ,  $^{99\text{m}}\text{Tc}$ , or  $^{211}\text{At}$ , all being radionuclides transported via NIS, in the culture medium for 6 h, or to various absorbed doses of  $^{123}\text{I}$  or  $^{131}\text{I}$  for 48 h. NIS mRNA expression was analyzed using quantitative reverse-transcriptase polymerase chain reaction. **Results:** Iodide transport and NIS mRNA expression were reduced by all radionuclides. At the same absorbed dose, iodide transport was reduced the most by  $^{211}\text{At}$ , followed by  $^{123}\text{I}$  and  $^{99\text{m}}\text{Tc}$  (equally potent), whereas  $^{131}\text{I}$  was least effective. The onset of NIS downregulation was rapid (<1 d after irradiation) in cells exposed to  $^{123}\text{I}$  or  $^{211}\text{At}$  and was delayed in cells irradiated with  $^{131}\text{I}$  or  $^{99\text{m}}\text{Tc}$ . Iodide transport and NIS expression were recovered only for  $^{211}\text{At}$ .  $^{123}\text{I}$  reduced the iodine transport and the NIS mRNA expression more efficiently than did  $^{131}\text{I}$  at an equivalent absorbed dose, with a relative biological effectiveness of about 5. **Conclusion:** The stunning effect per unit absorbed dose is more severe for  $^{123}\text{I}$  than for  $^{131}\text{I}$ . Despite the lower absorbed dose per unit activity for  $^{123}\text{I}$  than for  $^{131}\text{I}$ , stunning by  $^{123}\text{I}$  cannot be excluded in patients. The degree to which iodide transport capacity and NIS mRNA expression are reduced seems to be related to the biological effectiveness of the type of radiation delivering the absorbed dose to the target, with  $^{211}\text{At}$  (which has the highest relative biological effectiveness) causing the highest degree of stunning per unit absorbed dose in the present study.

**Key Words:** thyroid stunning; NIS;  $^{131}\text{I}$ ;  $^{123}\text{I}$ ;  $^{99\text{m}}\text{Tc}$ ;  $^{211}\text{At}$

*J Nucl Med* 2009; 50:1161–1167

DOI: 10.2967/jnumed.108.061150

**T**hyroid stunning is a complication of radiation therapy with  $^{131}\text{I}$ , the consequences of which affect mainly the management of thyroid carcinoma patients (1–6). The stunning phenomenon is characterized by less  $^{131}\text{I}$  uptake at therapy than was predicted from the  $^{131}\text{I}$  uptake measurement during dose planning. The reason for this effect is not fully understood, although several mechanisms have been proposed. One explanation, rejecting an effect from the diagnostic  $^{131}\text{I}$ , is that a low  $^{131}\text{I}$  content measured in treated tumors reflects a rapid loss of viable tissues and that dying cells damaged by irradiation are incapable of keeping accumulated iodide (7,8). In this case, thyroid stunning would be regarded as an artifact due to an early therapeutic effect of the ablative  $^{131}\text{I}$  and hence not a clinical problem. Another suggested mechanism originates from the hypothesis that irradiation might disturb the uptake of iodide per se independently of radiation effects on vital cell functions and thus before cell viability eventually is affected. This possibility is supported by experimental studies showing that thyrotropin-stimulated iodide transport mediated by the sodium iodide symporter (NIS) is markedly reduced when cultured thyroid cells are irradiated with relatively small  $^{131}\text{I}$  doses (0.15–3 Gy) equivalent to those estimated to be received after diagnostic administration of  $^{131}\text{I}$  *in vivo* (9,10). Moreover,  $^{131}\text{I}$  irradiation reduces expression of NIS at the transcriptional level in still-viable thyrocytes (11). Together, this suggests that stunning may result from a decreased synthesis of NIS leading to diminished amounts of iodide-transporting protein in preirradiated cells.

Thyroid stunning potentially threatens the effectiveness of a given ablative amount of  $^{131}\text{I}$ . To avoid this problem,  $^{123}\text{I}$  has been proposed to replace  $^{131}\text{I}$  for diagnostic uptake

Received Dec. 16, 2008; revision accepted Mar. 9, 2009.

For correspondence or reprints contact: Charlotta Lundh, Department of Radiation Physics, Sahlgrenska University Hospital, Göteborg University, SE-413 45, Göteborg, Sweden.

E-mail: [charlotta.lundh@radfys.gu.se](mailto:charlotta.lundh@radfys.gu.se)

COPYRIGHT © 2009 by the Society of Nuclear Medicine, Inc.

measurements. Stunning has nevertheless occurred in thyroid remnants and metastases after administration of  $^{123}\text{I}$  within a rather wide range of diagnostic activities (50–200 MBq) (7,12,13). However, whether  $^{123}\text{I}$  irradiation triggers cellular changes leading to loss of NIS expression and reduced iodide uptake has not been experimentally investigated. Likewise, it is not known if other radionuclides such as  $^{211}\text{At}$  and  $^{99\text{m}}\text{Tc}$ , which also accumulate in the thyroid by NIS-mediated uptake (14,15), may cause stunning.  $^{99\text{m}}\text{TcO}_4^-$  (pertechnetate) is routinely used in the functional evaluation of thyroid nodules and goiters.  $^{211}\text{At}$  is an  $\alpha$ -emitter suggested for therapy of poorly differentiated thyroid carcinoma (16,17) and non-thyroid tumors expressing NIS after gene transfer (18).

$^{99\text{m}}\text{Tc}$ ,  $^{211}\text{At}$ ,  $^{123}\text{I}$ , and  $^{131}\text{I}$  have different decay properties. The main part of the absorbed dose is deposited by particles, but the type of particle, the energy, and the yield differ considerably among these radionuclides. For example,  $\alpha$ -particles and Auger electrons characterized by high-linear-energy transfer and relative biological effectiveness (RBE) (19) are predominantly emitted by  $^{211}\text{At}$  and  $^{123}\text{I}$ , respectively. Thus, comparison of these nuclides to see which type of radiation is more prone to inducing stunning would be of interest. In this study, we therefore investigated first whether  $^{123}\text{I}$ ,  $^{99\text{m}}\text{Tc}$ , and  $^{211}\text{At}$  are able to induce stunning in vitro and second whether iodide transport and NIS messenger RNA (mRNA) expression might be affected differently by  $^{123}\text{I}$ ,  $^{99\text{m}}\text{Tc}$ , and  $^{211}\text{At}$  irradiation than by  $^{131}\text{I}$  irradiation analyzed at equivalent absorbed doses. To mimic internal radiation of the normal thyroid in vivo, quiescent ( $G_0$ ) primary thyroid cells cultured as a monolayer in bicameral chambers were continuously irradiated for 6 or 48 h while the nuclides were transported across the epithelium and gradually accumulated in the culture compartment corresponding to the follicular lumen.

## MATERIALS AND METHODS

### Cell Culture

Porcine thyroid primary cells, prepared as previously described (9), were plated on collagen-coated micropore filters (pore size, 0.4  $\mu\text{m}$ ) in bicameral chambers (Transwell, 3413; Corning Costar) and cultured for 7 d at 37°C in an incubator with 5%  $\text{CO}_2$  in Earle minimum essential medium supplemented with 5% fetal calf serum, penicillin (200 U/mL), streptomycin (200  $\mu\text{g}/\text{mL}$ ), and amphotericin B (2.5  $\mu\text{g}/\text{mL}$ ) (PAA Laboratories GmbH). The medium in the culture chamber was replaced every 2–3 d. At confluency, the growth of the proliferating cells was arrested and they established a tight monolayer, of which the barrier function was monitored by measuring transepithelial resistance with a Millicell-ERS ohmmeter (Millipore Corp.). The basal and apical compartments of the bicameral chamber correspond to the extrafollicular space and the follicular lumen, respectively (Fig. 1). All experiments were thus performed on confluent cells, of which most were postmitotic.

### Radionuclides

All iodine isotopes used ( $^{123}\text{I}$ ,  $^{125}\text{I}$ , and  $^{131}\text{I}$ ) were obtained as NaI (Nycomed Amersham, PLC).  $^{99\text{m}}\text{Tc}$  was obtained as pertechnetate,  $^{99\text{m}}\text{TcO}_4^-$ , by elution of a  $^{99}\text{Mo}/^{99\text{m}}\text{Tc}$  generator (UltraTechnekow

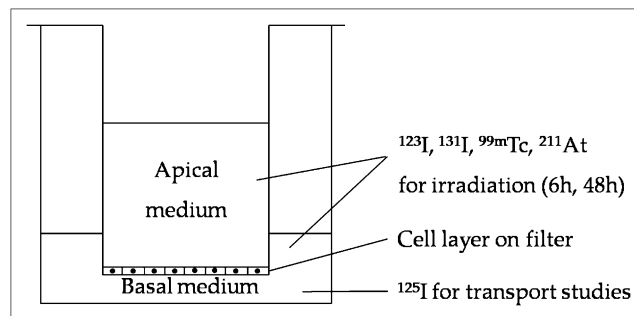


**FIGURE 1.** Transwell bicameral culture chamber system. Pig thyrocytes were grown on microporous filter (pore size, 0.4  $\mu\text{m}$ ) that divides well into apical and basal compartments corresponding to follicular lumen and extrafollicular space, respectively. Cells were irradiated with  $^{123}\text{I}$ ,  $^{131}\text{I}$ ,  $^{99\text{m}}\text{Tc}$ , or  $^{211}\text{At}$  in medium, both apically and basally. Gradual accumulation of radionuclide in apical culture medium due to NIS-mediated transport in basal-to-apical direction was taking place during irradiation. After irradiation, cell cultures were analyzed for  $^{125}\text{I}^-$  transport capacity ( $^{125}\text{I}^-$  was added basally), total DNA content, and NIS mRNA expression.

FM; Mallinckrodt Medical).  $^{211}\text{At}$  was produced at the Cyclotron and PET Unit at Rigshospitalet, Copenhagen, Denmark, by the  $^{209}\text{Bi}(\alpha,2n)^{211}\text{At}$  reaction, where the targets, aluminum backings with 19- to 24- $\mu\text{m}$   $^{209}\text{Bi}$  layers, were prepared at the Department of Physics, Chalmers University of Technology, Göteborg, Sweden.  $^{211}\text{At}$  was distilled according to methods previously described (20). The physical properties of the radionuclides are given in Table 1.

**TABLE 1.** Physical Properties of Radionuclides Studied (22)

Property	$^{99\text{m}}\text{Tc}$	$^{123}\text{I}$	$^{125}\text{I}$	$^{131}\text{I}$	$^{211}\text{At}$
Decay mode	IT	EC	EC	$\beta^-$	$\alpha$ , EC
Half-life	6.0 h	13 h	60 d	8.0 d	7.2 h
Radiation yield (%)					
Photon energy					
0–40 keV	7.9	95	160	5.5	18
40–100 keV	—	—	—	—	38
100–300 keV	87	83	—	6.1	—
>300 keV	—	—	—	88	—
Electron energy					
0–10 keV	220	280	600	8.0	9.4
10–20 keV	2.1	—	—	3.4	17
20–40 keV	—	12	33	7.4	—
40–100 keV	—	—	—	24	1.3
100–300 keV	11	16	—	48	—
300–600 keV	—	—	—	21	—
$\alpha$ -Particle energy					
5,000–6,000 keV	—	—	—	—	42
6,000–7,000 keV	—	—	—	—	0.63
7,000–8,000 keV	—	—	—	—	58

EC = electron capture; IT = isomeric transition.

$\alpha$ -Particles,  $\beta$ -particles, and atomic electrons are included. Photons with abundance  $\geq 5\%$  and electrons with abundance  $\geq 1\%$  are included.

### Absorbed Dose Calculations

Estimations of the absorbed dose to the cell layer from  $^{131}\text{I}$ ,  $^{123}\text{I}$ , or  $^{99\text{m}}\text{Tc}$  were based on Monte Carlo simulations with the PENELOPE code and PENCYL program (21), as described earlier (10). Radionuclide decay data were collected from *MIRD: Radionuclide Data and Decay Schemes* (22). The absorbed dose for  $^{211}\text{At}$  was calculated using the time integral of equilibrium dose rate from  $^{211}\text{At}$  in the basal and apical compartments. The increasing activity concentrations in the apical medium generated by ongoing trans-epithelial (from basal to apical) transport of the radionuclides during irradiation was taken into consideration.

### Irradiation Procedures

Before irradiation, cell cultures were stimulated with thyrotropin (1 mU/mL; Sigma-Aldrich Sweden AB) for 48 h to upregulate the NIS expression and iodide transport capacity. Thyrotropin stimulation of cell cultures was maintained until iodide transport was evaluated.

Irradiation was performed mainly in accordance with the protocols of earlier studies (9–11). Two types of experiments were investigated: a comparison of the effects of a standardized dose (0.5 Gy) from  $^{99\text{m}}\text{Tc}$ ,  $^{123}\text{I}$ ,  $^{131}\text{I}$ , or  $^{211}\text{At}$ , and a comparison of the dose–response relationship between  $^{123}\text{I}$  and  $^{131}\text{I}$  irradiation. In the first setup, culture medium containing  $^{99\text{m}}\text{Tc}$  (9.7 MBq/mL),  $^{123}\text{I}$  (7.8 MBq/mL),  $^{131}\text{I}$  (0.63 MBq/mL), or  $^{211}\text{At}$  (22 kBq/mL) was added to the bicameral chambers, both apically (200  $\mu\text{L}$ ) and basally (400  $\mu\text{L}$ ) (Fig. 1). The mean absorbed dose to the cells was 0.5 Gy after 6 h of exposure. The short exposure time was chosen to keep the change in dose rate low for the short-lived radionuclides  $^{99\text{m}}\text{Tc}$  and  $^{211}\text{At}$  (physical half-life, 6.0 and 7.2 h, respectively). In the second setup, cell cultures were irradiated with various activity concentrations of  $^{123}\text{I}$  (0.034–40 MBq/mL) and  $^{131}\text{I}$  (0.20–2.0 MBq/mL) for 48 h to mimic the longer exposure assumed for the thyroid in vivo. The activity of the medium added apically (100  $\mu\text{L}$ ) and basally (500  $\mu\text{L}$ ) resulted in an absorbed dose to the cell layer of 0.01–14 Gy and 2.9–14 Gy for  $^{123}\text{I}$  and  $^{131}\text{I}$ , respectively.

Organification of radioiodine was prevented by adding methimazole (1 mmol/L; Sigma-Aldrich Sweden AB) to the culture medium in all radiation experiments. Culture plates, one for each radionuclide and absorbed dose, were kept shielded by lead in the  $\text{CO}_2$  incubator at 37°C to prevent external cross irradiation between groups. Accidentally damaged or leaky cultures unable to concentrate radionuclide in the apical culture compartment during ongoing irradiation were identified by medium sampling and counting of activity content in the apical and the basal medium after exposure and were excluded. Irradiation was stopped by washing the cells in radionuclide-free medium at least 3 times before further culturing. None of the radionuclide used for irradiation of the cell culture remained after washing.

### $^{125}\text{I}^-$ Transport Studies

The transepithelial iodide transport capacity in irradiated and corresponding control cultures was evaluated using  $^{125}\text{I}^-$  as tracer. The basal medium was replaced with medium containing  $^{125}\text{I}^-$  (60 kBq/mL), and after transport had been allowed for 30 min at 37°C, 50- $\mu\text{L}$  samples were taken from both the apical and the basal compartments. The activity in the samples was measured with a  $\gamma$ -counter (Wallac 1480 WIZARD 3"; Wallac Oy). Corrections were made, when necessary, for radioactive decay and background. The relative  $^{125}\text{I}^-$  transport through the cell layer, defined as the ratio between the amount of  $^{125}\text{I}^-$  transported by the irradiated cell

cultures and that transported by the nonirradiated control cells, was determined. The same cultures were subjected to repeated  $^{125}\text{I}^-$  transport studies to monitor iodide transport changes over time. After each transport study, the cell cultures were washed with fresh medium containing no radionuclides and then reincubated until the next transport study. The repeated short exposure to  $^{125}\text{I}^-$ , for about 30 min, in each transport measurement did not affect the basal transport rate as compared with that measured in matching non-irradiated cells (data not shown). The experiments were reproducible, and each group consisted of 3–6 cell cultures.

### Quantitative Reverse-Transcriptase Polymerase Chain Reaction (qRT-PCR) Analysis of NIS mRNA Expression

NIS transcript levels were quantified by qRT-PCR using a previously established protocol (11). Total RNA was extracted from the cell cultures using the RNeasy Micro Kit (Qiagen GmbH). The RNA was quantified with spectrophotometry at 260 nm, and 0.5  $\mu\text{g}$  was used for each sample to synthesize complementary DNA with random hexamers and TaqMan Reverse Transcription Reagents (Applied Biosystems). Primers to the porcine NIS gene and 18S (reference gene) were designed with the Primer Express Software (Applied Biosystems) according to the following templates: porcine NIS forward primer was 5'-ctctcctggcaggccatctct-3'; porcine NIS reverse primer was 5'-gctgagggtgccgtgta-3'; 18S forward primer was 5'-gtaaccctgtgaaccatt-3'; and 18S reverse primer was 5'-ccatcaatcggtagtagcg-3' (TAG Copenhagen A/S). The relative amounts of polymerase chain reaction products were quantified using QuantiTect SYBR Green (Promega) and the ABI PRISM 7900HT Sequence Detection System (Applied Biosystems). The thermal cycling conditions were an initial cycle of 2 min at 50°C, a 15-min cycle at 95°C, 40 cycles of 15 s each at 94°C (denaturation), and a cycle of 1 min at 60°C (annealing and extension). All amplification reactions were done in triplicate. The threshold cycle values were used for calculation of the relative RNA expression ratios between control and treated cell samples, according to Pfaffl (23).

### Cell Number Quantification

To rule out the possibility that any findings were related to altered cell number (i.e., due to loss of radiation-damaged cells), the total DNA content of cultures exposed to radionuclides was measured using a fluorometric DNA assay (24). The viability of the cells was monitored by iodide transport studies.

### Statistical Analysis

Results from iodide transport studies are given as mean  $\pm$  SEM in the figures. The Student *t* test was used to determine the statistical significance of differences between data obtained from the experimental groups.  $P < 0.05$  was considered significant. NIS mRNA data from qRT-PCR analyses were evaluated with the relative expression software tool (23).  $P < 0.001$  was considered statistically significant.

## RESULTS

Thyrotropin-stimulated thyroid cell monolayers were irradiated with  $^{123}\text{I}$ ,  $^{131}\text{I}$ ,  $^{99\text{m}}\text{Tc}$ , or  $^{211}\text{At}$  in the culture medium for 6 h, resulting in a standardized absorbed dose of 0.5 Gy. During exposure, the radionuclides were actively transported across the cell layer resulting in different apical-to-basal activity concentration ratios at the end of irradiation (6.0 for

$^{125}\text{I}$ , adopted for  $^{123}\text{I}$  and  $^{131}\text{I}$ ; 8.5 for  $^{211}\text{At}$ ; and 14 for  $^{99\text{m}}\text{Tc}$ ). These results were considered in the dosimetric calculations.

As shown in Figure 2, the transepithelial transport of iodide (monitored by  $^{125}\text{I}^-$ ) was reduced by all radionuclides studied. In general, the transport started to decrease 1–2 d after irradiation and was suppressed most significantly after 5–7 d. Immediately after irradiation, a higher transport capacity was shown by the cell cultures than by nonirradiated control cells. This was, however, statistically significant only for  $^{211}\text{At}$ -irradiated cultures. At the given absorbed dose (0.5 Gy), the strongest inhibitory effect on iodide transport, amounting to nearly 70% of the control level, was observed in  $^{211}\text{At}$ -irradiated cells.  $^{123}\text{I}$  and  $^{99\text{m}}\text{Tc}$  were equally potent and decreased iodide transport by 30%–40%, whereas  $^{131}\text{I}$ -irradiated cells reduced transport by less than 20%. Interestingly, whereas no significant recovery from stunning was evident in cultures exposed to  $^{131}\text{I}$ ,  $^{123}\text{I}$ , or  $^{99\text{m}}\text{Tc}$ , iodide transport was statistically significantly increased between 5 and 7 d in cells that had been irradiated with  $^{211}\text{At}$  (Fig. 2).

The expression of NIS mRNA was investigated in cell cultures that were irradiated in parallel with those analyzed for changes in  $^{125}\text{I}^-$  transport. Similar to the effects on iodide transport, the smallest and largest reduction of NIS transcript levels were evident in cells exposed to  $^{131}\text{I}$  and  $^{211}\text{At}$ , respectively. However, several additional differences were observed. Most strikingly,  $^{123}\text{I}$  and  $^{211}\text{At}$  had already suppressed the NIS expression 24 h after irradiation, whereas the suppression was delayed in cells exposed to  $^{131}\text{I}$  and  $^{99\text{m}}\text{Tc}$ . Moreover, the NIS transcript level recovered completely in cells exposed to  $^{123}\text{I}$  and partially in cells exposed to  $^{211}\text{At}$  after culture for 5 d after irradiation (Fig. 3 and Table 2). NIS expression did not recover in cells exposed to  $^{131}\text{I}$  or  $^{99\text{m}}\text{Tc}$  during the interval studied.

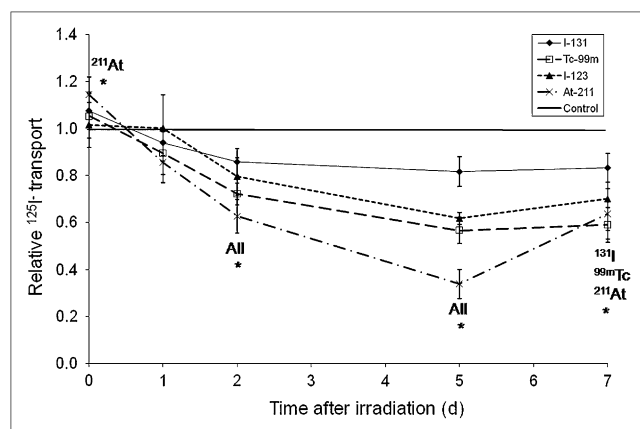


**FIGURE 2.** Time-dependent iodide ( $^{125}\text{I}^-$ ) transport changes in filter-cultured thyrocytes after irradiation with  $^{123}\text{I}$ ,  $^{131}\text{I}$ ,  $^{99\text{m}}\text{Tc}$ , or  $^{211}\text{At}$  to 0.5 Gy for 6 h. Effects of irradiation are presented relative to transport level monitored in nonirradiated cultures at each time point. Results are given as mean  $\pm$  SEM ( $n = 6$ ). \*Statistically significant difference from controls,  $P < 0.05$ .

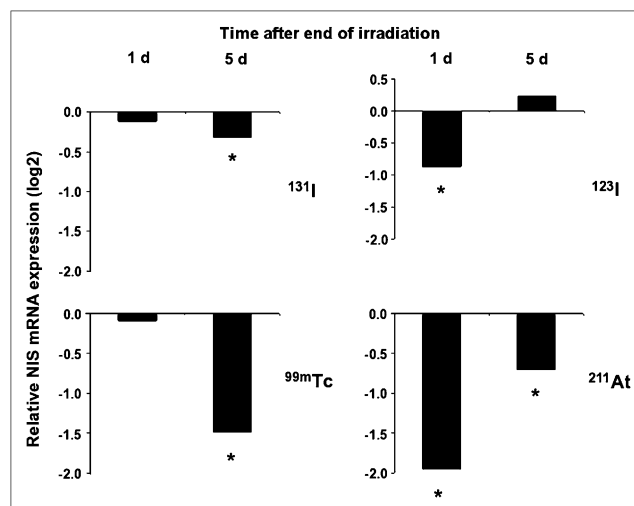


**FIGURE 3.** Changes of NIS mRNA expression in thyroid cells irradiated with  $^{123}\text{I}$ ,  $^{131}\text{I}$ ,  $^{99\text{m}}\text{Tc}$ , or  $^{211}\text{At}$  at same dose (0.5 Gy) and exposure times as shown in Figure 2 (representing data from parallel cultures in same experiments) on days 1 and 5 after irradiation. qRT-PCR data are presented as log<sub>2</sub> expression levels compared with those of matched nonirradiated controls ( $n = 3$ ). \*Statistically significant difference from controls,  $P < 0.001$ .

The effects of  $^{131}\text{I}$  and  $^{123}\text{I}$  on thyrotropin-stimulated iodide transport were compared in dose-response experiments after irradiation for 48 h (Fig. 4).  $^{131}\text{I}$  reduced the transepithelial  $^{125}\text{I}^-$  transport, in an absorbed dose-dependent manner, by approximately 30% at 2.7 Gy and 85% at 13 Gy (Fig. 4). Significantly lower absorbed doses of  $^{123}\text{I}$  were required to induce a corresponding reduction of iodide transport.

All experiments were performed on confluent and growth-arrested (i.e., G<sub>0</sub>) cells. There were no significant changes in DNA content between nonirradiated and irradiated cultures either immediately or 5 d after radionuclide exposure (data not shown), indicating that the total cell number was not influenced by the irradiation.

**TABLE 2.** Changes of NIS mRNA Expression in Thyroid Cells Irradiated with  $^{123}\text{I}$ ,  $^{131}\text{I}$ ,  $^{99\text{m}}\text{Tc}$ , or  $^{211}\text{At}$  to Absorbed Dose of 0.5 Gy During 6 Hours, on Days 1 and 5 After Irradiation

Radionuclide	NIS mRNA downregulation (% of control)	
	1 d	5 d
$^{131}\text{I}$	NS	80
$^{123}\text{I}$	55	NS
$^{99\text{m}}\text{Tc}$	NS	34
$^{211}\text{At}$	26	61

qRT-PCR data are presented as percentage downregulation, compared with matched nonirradiated controls. NS indicates no statistically significant difference from controls,  $P < 0.001$ .

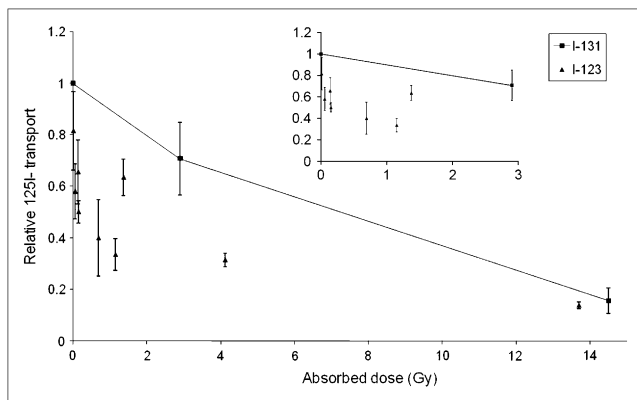


**FIGURE 4.** Dose-dependent iodide ( $^{125}\text{I}^-$ ) transport changes in filter-cultured thyroid cells irradiated with  $^{131}\text{I}$  or  $^{123}\text{I}$  for 48 h. Effect on transport was evaluated 3 d after end of radionuclide exposure. Results obtained from 3 separate experiments, with triplicates in each, are given relative to matching nonirradiated controls as mean  $\pm$  SEM ( $n = 3$ ). Inset shows details at low absorbed doses.

## DISCUSSION

Four radionuclides,  $^{123}\text{I}$ ,  $^{131}\text{I}$ ,  $^{99\text{m}}\text{Tc}$ , and  $^{211}\text{At}$ , known to be concentrated in the thyroid by NIS-mediated transport were compared for their ability to induce thyroid stunning in vitro at a standardized exposure time (6 h) and absorbed dose (0.5 Gy). All were found to inhibit iodide transport in cultured thyroid cells 1–5 d after the irradiation. The potency to induce stunning differed significantly ( $^{131}\text{I} < ^{99\text{m}}\text{Tc} = ^{123}\text{I} < ^{211}\text{At}$ ), ranging from 20%–80% transport inhibition (Fig. 2). This difference was evident also when the maximal downregulation of NIS expression was compared by qRT-PCR analysis (Fig. 3). Interestingly, the decrease in NIS transcription was much faster in cells irradiated with  $^{211}\text{At}$  or  $^{123}\text{I}$ , already appearing after 1 d, than in cells exposed to  $^{99\text{m}}\text{Tc}$  or  $^{131}\text{I}$ . The response to  $^{211}\text{At}$  and  $^{123}\text{I}$  also differed from the response to the other 2 radionuclides in that NIS expression and iodide transport partly recovered within 5 d after irradiation. Decreased expression of NIS at the transcriptional level seems to be a common mechanism leading to inhibited iodide transport. However, the magnitude and kinetics of radiation-induced stunning differ between the radionuclides studied, probably because of the different physical properties of the radionuclides (Table 1).

RBE is defined as the ratio of the absorbed doses, from a reference radiation type (usually photons) and a test radiation that causes equal biologic effect (19). Low-energy electrons ( $E \leq 50$  keV) such as Auger electrons and  $\alpha$ -particles ionize matter more densely than do photons or conventional electrons with higher energy, resulting in higher RBE. Auger electrons have RBE values of 1.5–40 depending on the electron energy and the location of the radionuclide, because of the limited range of these particles (25). Likewise, reported RBE values for the  $\alpha$ -particle emitter  $^{211}\text{At}$  vary between 1.5 and 25 for different tissues, experimental con-

ditions, and endpoints (26–33). In the present study, the dose-response curves presented in Figure 4 allow an estimation of RBE (at the absorbed dose levels required to reduce the relative  $^{125}\text{I}$  transport by 1 natural log, 37%) for the stunning effect induced by  $^{123}\text{I}$ , compared with  $^{131}\text{I}$ , which was about 5 (estimated from Fig. 4). RBE for stunning could, however, not be determined for the other radionuclides according to the strict definition. However, at 5 d after irradiation (Fig. 2), which probably is close to the time at which the maximal inhibitory effects of the nuclides on iodide transport are monitored,  $^{211}\text{At}$  was 2.4 times more efficient than  $^{131}\text{I}$  and 1.7 times more efficient than  $^{99\text{m}}\text{Tc}$  in inducing stunning.

$^{99\text{m}}\text{Tc}$  and  $^{123}\text{I}$  emit relatively low-energy electrons that are responsible for most of the absorbed dose to the cells, compared with  $^{131}\text{I}$ , for which more than 90% of the absorbed dose is delivered by higher-energy electrons (Table 1). The effectiveness of  $^{99\text{m}}\text{Tc}$  and  $^{123}\text{I}$  in causing stunning was similar, although NIS expression was downregulated more quickly by  $^{123}\text{I}$  than by  $^{99\text{m}}\text{Tc}$ . It is reasonable to assume that the relatively poor stunning effect of  $^{131}\text{I}$ , compared with  $^{123}\text{I}$  or  $^{99\text{m}}\text{Tc}$ , depends on the fact that the latter have a higher abundance of low-energy electrons (0–10 keV) that might give rise to more complex DNA lesions. This explanation requires that the radionuclide be transported closely to the cell nucleus.

The different dose rates from the investigated nuclides might also influence the cellular responses to irradiation.  $^{99\text{m}}\text{Tc}$  and  $^{211}\text{At}$  had initially the highest dose rate, their half-life being close to the total exposure time, resulting in about a 50% reduction in dose rate during exposure. In contrast, the long half-life of  $^{131}\text{I}$  made the dose rate relatively stable during the irradiation period. The higher dose rate can thus be responsible at least in part for the fast downregulation of the NIS-mRNA expression in cells irradiated with  $^{211}\text{At}$  or  $^{123}\text{I}$ . The relatively slow response to  $^{99\text{m}}\text{Tc}$  must, however, have another explanation.  $^{99\text{m}}\text{Tc}$  was transported twice as quickly across the epithelial cell layer as the other radionuclides. The reason for this difference is unknown, although previous studies comparing transport of  $^{125}\text{I}^-$  and  $^{211}\text{At}$  suggest different transport properties between radionuclides concentrated in thyroid cells (14,34). A short intracellular transit time decreases the probability that low-energy electrons from  $^{99\text{m}}\text{Tc}$  reach the cell nucleus, eventually leading to less or delayed interference with the transcriptional machinery regulating NIS. In addition, a lower emission yield of electrons in the range of 20–40 keV might further weaken the transcriptional response to  $^{99\text{m}}\text{Tc}$  relative to that of  $^{123}\text{I}$ .

The decrease in NIS mRNA levels was rapid, preceding the earliest signs of inhibited iodide transport, in  $^{211}\text{At}$ - and  $^{123}\text{I}$ -irradiated cells. We have previously shown that loss of iodide transport accompanies downregulation of NIS also in cells irradiated with  $^{131}\text{I}$  at a higher dose (7.5 Gy) than used here (11). Although other mechanisms, that is, posttranscriptional, may contribute, the suggestion is strong that reduced transcriptional activity of the NIS promoter is a key feature leading to stunning in normal thyroid cells.

Notably, the half-time of native NIS protein—estimated at 3 d in thyrotropin-starved cells and 5 d after thyrotropin stimulation—is unusually long (35). The slow turnover of NIS probably reflects a mechanism by which newly synthesized NIS is retained in the plasma membrane. Such a mechanism might be of physiologic importance in keeping a high iodide uptake capacity although other thyroid functions may fluctuate. It will thus take a considerable time for a reduced NIS gene expression to be translated into a decreased number of functionally active NIS molecules at the cell surface. Therefore, it is not surprising that radiation-induced loss of iodide transport develops gradually and rather slowly after the NIS gene transcription is significantly suppressed. Moreover, these *in vitro* findings support the many clinical reports of a delay in detection of stunning until several days after the administration of radioiodine for diagnostic purposes (1–7,36,37).

A central question not previously investigated is whether thyroid stunning is irreversible, being part of a general stress response to radiation-induced damage that eventually is lethal, or whether iodide transport may recover in the affected cell. Clinical studies indicate that stunning is a prolonged effect lasting for many days (1,3,6,7,36). This finding was confirmed in the present study, in which no signs of recovery of the suppressed iodide transport were observed in cultures exposed to  $^{131}\text{I}$  or  $^{99\text{m}}\text{Tc}$  up to 1 wk after the irradiation period. It was therefore surprising that the  $^{211}\text{At}$ -irradiated cells regained iodide transport capacity, accompanied by a partial normalization of the NIS transcript level. As clear signs of recovery of the NIS expression also were noted in cells exposed to  $^{123}\text{I}$ , it is tempting to speculate that early recovery from stunning might require that the NIS down-regulation be rapidly triggered by high-linear-energy-transfer radiation. This possibility further suggests, assuming that loss of NIS expression directly or indirectly is part of a transcriptional response to irradiation-induced DNA damage, that the incidence and type of DNA lesions and the efficiency with which DNA repair mechanisms are activated determine the kinetics of stunning. However, no statistically significant recovery was seen for  $^{99\text{m}}\text{Tc}$ -irradiated cells even though the emission profile is quite similar to that of  $^{123}\text{I}$ . This difference may be due to the shorter transit time of  $^{99\text{m}}\text{Tc}$ . This shorter transit time is demonstrated by the higher apical-to-basal activity concentration ratio at the end of irradiation for  $^{99\text{m}}\text{Tc}$  (14), compared with  $^{123}\text{I}$  (6.0). Although the recovery mechanism is yet to be elucidated, this finding is intriguing as it indicates that stunning is not a static process but can be modulated. Moreover, because the observations were made on postmitotic cells that did not change in number during or after irradiation, it is the actual irradiated cells that recover from stunning, with little or no contribution from cell renewal.

$^{123}\text{I}$  has to some extent started to replace  $^{131}\text{I}$  for dose planning before  $^{131}\text{I}$  therapy in thyroid cancer, partly because its preferable photon energy results in a superior quality of scintigraphic images, but mainly because it is supposed to not

cause stunning. For dose planning, an activity of 74–370 MBq of  $^{131}\text{I}$  is usually administered, compared with 10–200 MBq of  $^{123}\text{I}$  (1,6,7,13,36–39). According to Johansson et al. (40), the absorbed dose per unit activity is 490 and 5 mGy/MBq to the thyroid gland from  $^{131}\text{I}$  and  $^{123}\text{I}$ , respectively. Thus, the absorbed dose per unit activity in the thyroid is about 100 times lower from  $^{123}\text{I}$  than from  $^{131}\text{I}$ . Although this factor is smaller in smaller targets such as thyroid remnants and metastases, because of the lower absorbed fraction of the electrons from  $^{131}\text{I}$ ,  $^{123}\text{I}$  would be preferable to avoid stunning. In this study, we show that iodide transport in cultured thyroid cells is reduced about twice as much by  $^{123}\text{I}$  as by  $^{131}\text{I}$  per unit of absorbed dose. This finding may explain why stunning may yet occur when  $^{123}\text{I}$  is used for dose planning, as recently reported in some clinical studies (7,12,13).

## CONCLUSION

$^{123}\text{I}$  causes a more severe stunning effect per unit absorbed dose than does  $^{131}\text{I}$ , with an RBE value of about 5. Although the absorbed dose to the thyroid gland per unit activity is only 1/100 of that delivered by  $^{131}\text{I}$ , and somewhat higher in small thyroid remnants and metastases, stunning due to  $^{123}\text{I}$  cannot be excluded in patients. The degree of the reduction in iodide transport capacity seems to be related to the biologic effectiveness of the type of radiation delivering the absorbed dose to the target, with  $^{211}\text{At}$  causing the highest degree of stunning per unit absorbed dose in the present study.

## ACKNOWLEDGMENTS

We acknowledge Johanna Dalmo for supplying  $^{131}\text{I}$ , and we acknowledge Dr. Sture Lindegren at the Department of Radiation Physics, Göteborg University, and Dr. Holger Jensen at the PET and Cyclotron Unit at Rigshospitalet, Copenhagen, for supplying  $^{211}\text{At}$ . This study was supported by grants 3427 and 4567 from the Swedish Cancer Society, by the Swedish Radiation Protection Authority, by grant 537 from the Swedish Research Council, and by the King Gustav V Jubilee Clinic Cancer Research Foundation.

## REFERENCES

- Jeevanram RK, Shah DH, Sharma SM, Ganatra RD. Influence of initial large dose on subsequent uptake of therapeutic radioiodine in thyroid cancer patients. *Int J Rad Appl Instrum B*. 1986;13:277–279.
- McDougall IR. 74 MBq radioiodine  $^{131}\text{I}$  does not prevent uptake of therapeutic doses of  $^{131}\text{I}$  (i.e. it does not cause stunning) in differentiated thyroid cancer. *Nucl Med Commun*. 1997;18:505–512.
- Bajén MT, Mañé S, Muñoz A, Ramón García J. Effect of diagnostic dose of 185 MBq  $^{131}\text{I}$  on postsurgical thyroid remnants. *J Nucl Med*. 2000;41:2038–2042.
- Dam HQ, Kim SM, Lin HC, Intenzo CM.  $^{131}\text{I}$  therapeutic efficacy is not influenced by stunning after diagnostic whole-body scanning. *Radiology*. 2004;232:527–533.
- Kalinyak JE, McDougall IR. Whole-body scanning with radionuclides of iodine, and the controversy of “thyroid stunning.” *Nucl Med Commun*. 2004;25:883–889.
- Lassmann M, Luster M, Hänischied H, Reiners C. Impact on  $^{131}\text{I}$  diagnostic activities on the biokinetics of thyroid remnants. *J Nucl Med*. 2004;45:619–625.
- Hilditch TE, Dempsey MF, Bolster AA, McMenemin RM, Reed NS. Self-stunning in thyroid ablation: evidence from comparative studies of diagnostic  $^{131}\text{I}$  and  $^{123}\text{I}$ . *Eur J Nucl Med Mol Imaging*. 2002;29:783–788.

8. Sisson JC, Avram AM, Lawson SA, Gauger PG, Doherty GM. The so-called stunning of thyroid tissue. *J Nucl Med.* 2006;47:1406–1412.
9. Postgård P, Himmelman J, Lindencrona U, et al. Stunning of iodide transport by  $^{131}\text{I}$  irradiation in cultured thyroid epithelial cells. *J Nucl Med.* 2002;43:828–834.
10. Lundh C, Nordén M, Nilsson M, Forssell-Aronsson E. Reduced iodide transport (stunning) and DNA synthesis in thyrocytes exposed to low absorbed doses from  $^{131}\text{I}$  in vitro. *J Nucl Med.* 2007;48:481–486.
11. Nordén MM, Larsson F, Tedelind S, et al. Down-regulation of the sodium/iodide symporter explains  $^{131}\text{I}$ -induced thyroid stunning. *Cancer Res.* 2007;67:7512–7517.
12. Cohen JB, Kalinyak JE, McDougall IR. Clinical implications of the differences between diagnostic  $^{123}\text{I}$  and post-therapy  $^{131}\text{I}$  scans. *Nucl Med Commun.* 2004;25:129–134.
13. Urhan M, Dadparvar S, Mavi A, et al. Iodine-123 as a diagnostic imaging agent in differentiated thyroid carcinoma: a comparison with iodine-131 post-treatment scanning and serum thyroglobulin measurement. *Eur J Nucl Med Mol Imaging.* 2007;34:1012–1017.
14. Lindencrona U, Nilsson M, Forssell-Aronsson E. Similarities and differences between free  $^{211}\text{At}$  and  $^{125}\text{I}$ - transport in porcine thyroid epithelial cells cultured in bicameral chambers. *Nucl Med Biol.* 2001;28:41–50.
15. Zuckier LS, Dohan O, Li Y, Chang CJ, Carrasco N, Dadachova E. Kinetics of perchlorate uptake and comparative biodistribution of perchlorate, pertechnetate, and iodide by NaI symporter-expressing tissues in vivo. *J Nucl Med.* 2004;45:500–507.
16. Zalutsky MR, Vaidyanathan G. Astatine-211-labeled radiotherapeutics: an emerging approach to targeted alpha-particle radiotherapy. *Curr Pharm Des.* 2000;6:1433–1455.
17. Lundh C, Lindencrona U, Schmitt A, Nilsson M, Forssell-Aronsson E. Biodistribution of free  $^{211}\text{At}$  and  $^{125}\text{I}$ - in nude mice bearing tumors derived from anaplastic thyroid carcinoma cell lines. *Cancer Biother Radiopharm.* 2006;21:591–600.
18. Carlin S, Mairs RJ, Welsh P, Zalutsky MR. Sodium-iodide symporter (NIS)-mediated accumulation of [ $^{211}\text{At}$ ]astatide in NIS-transfected human cancer cells. *Nucl Med Biol.* 2002;29:729–739.
19. ICRP Publication 92: *Relative Biological Effectiveness (RBE), Quality Factor (Q), and Radiation Weighting Factor ( $w_R$ )*. Kidlington, U.K.: International Commission on Radiological Protection; 2003.
20. Lindegren S, Bäck T, Jensen HJ. Dry-distillation of astatine-211 from irradiated bismuth targets: a time-saving procedure with high recovery yields. *Appl Radiat Isot.* 2001;55:157–160.
21. Salvat F, Fernández-Varea JM, Acosta E, Sempau J. *PENELOPE: A Code System for Monte Carlo Simulation of Electron and Photon Transport*. Issy-les-Moulineaux, France: OECD Nuclear Energy Agency; 2001.
22. Weber DA, Eckerman KF, Dillman LT, Ryman JC. *MIRD: Radionuclide Data and Decay Schemes*. Reston, VA: Society of Nuclear Medicine; 1989.
23. Pfaffl MW, Horgan GW, Dempfle L. Relative expression software tool (REST) for group-wise comparison and statistical analysis of relative expression results in real-time PCR. *Nucleic Acids Res.* 2002;30:e36.
24. Labarca C, Paigen K. A simple, rapid, and sensitive DNA assay procedure. *Anal Biochem.* 1980;102:344–352.
25. Fairlie I. RBE and  $w_R$  values of Auger emitters and low-range beta emitters with particular reference to tritium. *J Radiol Prot.* 2007;27:157–168.
26. Harrison A, Royle L. Determination of absorbed dose to blood, kidneys, testes and thyroid in mice injected with  $^{211}\text{At}$  and comparison of testes mass and sperm number in x-irradiated and  $^{211}\text{At}$  treated mice. *Health Phys.* 1984;46:377–383.
27. Kassis AI, Harris CR, Adelstein SJ, Ruth TJ, Lambrecht R, Wolf AP. The in vitro radiobiology of astatine-211 decay. *Radiat Res.* 1986;105:27–36.
28. Aurlien E, Larsen RH, Akabani G, Olsen DR, Zalutsky MR, Bruland OS. Exposure of human osteosarcoma and bone marrow cells to tumour-targeted alpha-particles and gamma-irradiation: analysis of cell survival and microdosimetry. *Int J Radiat Biol.* 2000;76:1129–1141.
29. Palm S, Bäck T, Claesson I, et al. Effects of the alpha-particle emitter  $^{211}\text{At}$  and low-dose-rate gamma-radiation on the human cell line Colo-205 as studied with a growth assay. *Anticancer Res.* 1998;18:1671–1676.
30. Palm S, Andersson H, Bäck T, et al. In vitro effects of free  $^{211}\text{At}$ ,  $^{211}\text{At}$ -albumin and  $^{211}\text{At}$ -monoclonal antibody compared to external irradiation on two human cancer cell lines. *Anticancer Res.* 2000;20:1005–1012.
31. Elgqvist J, Berhardt P, Hultborn R, et al. Myelotoxicity and RBE of  $^{211}\text{At}$ -conjugated monoclonal antibodies compared with  $^{99m}\text{Tc}$ -conjugated monoclonal antibodies and  $^{60}\text{Co}$  irradiation in nude mice. *J Nucl Med.* 2005;46:464–471.
32. Bäck T, Andersson H, Divgi CR, et al.  $^{211}\text{At}$  radioimmunotherapy of subcutaneous human ovarian cancer xenografts: evaluation of relative biologic effectiveness of an  $\alpha$ -emitter in vivo. *J Nucl Med.* 2005;46:2061–2067.
33. Claesson AK, Stenerlöw B, Jacobsson L, Elmroth K. Relative biological effectiveness of the alpha-particle emitter  $^{211}\text{At}$  for double-strand break induction in human fibroblasts. *Radiat Res.* 2007;167:312–318.
34. Lindencrona U, Forssell-Aronsson E, Nilsson M. Transport of free  $^{211}\text{At}$  and  $^{125}\text{I}$ - in thyroid epithelial cells: effects of anion channel blocker 4,4'-diisothiocyanosulfonate-2,2'-disulfonic acid on apical efflux and cellular retention. *Nucl Med Biol.* 2007;34:523–530.
35. Riedel C, Levy O, Carrasco N. Post-transcriptional regulation of the sodium/iodide symporter by thyrotropin. *J Biol Chem.* 2001;276:21458–21463.
36. Leger FA, Izembart M, Dagoussset F, et al. Decreased uptake of therapeutic doses of iodine-131 after 185-MBq iodine-131 diagnostic imaging for thyroid remnants in differentiated thyroid carcinoma. *Eur J Nucl Med.* 1998;25:242–246.
37. Park H-M, Perkins OW, Edmondson JW, Schnute RB, Manatunga A. Influence of diagnostic radioiodines on the uptake of ablative dose of iodine-131. *Thyroid.* 1994;4:49–54.
38. Klein HA, DiSibio KJ, Sims D, Singleton HC, Worthy LJ. I-123 whole body scanning: case report and discussion. *Clin Nucl Med.* 2005;30:312–316.
39. Silberstein EB. Comparison of outcomes after  $^{123}\text{I}$  versus  $^{131}\text{I}$  preablation imaging before radioiodine ablation in differentiated thyroid carcinoma. *J Nucl Med.* 2007;48:1043–1046.
40. Johansson L, Leide-Svegborn S, Mattsson S, Nosslin B. Biokinetics of iodide in man: refinement of current ICRP dosimetry models. *Cancer Biother Radiopharm.* 2003;18:445–450.



The Journal of  
NUCLEAR MEDICINE

## Radiation-Induced Thyroid Stunning: Differential Effects of $^{123}\text{I}$ , $^{131}\text{I}$ , $^{99\text{m}}\text{Tc}$ , and $^{211}\text{At}$ on Iodide Transport and NIS mRNA Expression in Cultured Thyroid Cells

Charlotta Lundh, Ulrika Lindencrona, Per Postgård, Therese Carlsson, Mikael Nilsson and Eva Forssell-Aronsson

*J Nucl Med.* 2009;50:1161-1167.

Published online: June 12, 2009.

Doi: 10.2967/jnumed.108.061150

---

This article and updated information are available at:

<http://jnm.snmjournals.org/content/50/7/1161>

---

Information about reproducing figures, tables, or other portions of this article can be found online at:

<http://jnm.snmjournals.org/site/misc/permission.xhtml>

Information about subscriptions to JNM can be found at:

<http://jnm.snmjournals.org/site/subscriptions/online.xhtml>

*The Journal of Nuclear Medicine* is published monthly.  
SNMMI | Society of Nuclear Medicine and Molecular Imaging  
1850 Samuel Morse Drive, Reston, VA 20190.  
(Print ISSN: 0161-5505, Online ISSN: 2159-662X)

© Copyright 2009 SNMMI; all rights reserved.

The logo for the Society of Nuclear Medicine and Molecular Imaging (SNMMI) features the letters 'S', 'N', 'M', and 'I' in a stylized, overlapping arrangement. The 'S' and 'N' are in the top row, and the 'M' and 'I' are in the bottom row. The letters are white with a red outline, set against a red background.  
SOCIETY OF  
NUCLEAR MEDICINE  
AND MOLECULAR IMAGING